P14.6 THE DIURNAL CYCLE OF PRECIPITATION IN RADAR OBSERVATIONS, MODEL FORECASTS AND MAPLE NOWCASTS

Madalina Surcel[1*], Marc Berenguer[1], Isztar Zawadzki[1], Ming Xue[2,3] and Fanyou Kong[3]
(1) Department of Atmospheric and Oceanic Sciences, McGill University, Montreal, Canada
(2) School of Meteorology, University of Oklahoma, Norman, Oklahoma
(3) Center for Analysis and Prediction of Storms, University of Oklahoma, Norman, Oklahoma

1. INTRODUCTION

We have seen in a recent paper (Surcel et al., 2009) that the diurnal cycle of precipitation over the continental US exhibits some seasonal variability. This is a consequence of the fact that during the summer, precipitation is strongly forced by the diurnal cycle of solar heating and it usually initiates as small scales, while during spring, precipitation occurs at larger scales, being synoptically forced. Surcel et al. (2009) also showed that the ability of a convection parameterized, numerical weather prediction (NWP) model to depict the diurnal cycle of precipitation also varies with season showing more skill during spring.

Here, we add to the previous work, the evaluation of precipitation forecasts from two other models. The differences in performance between models are indicative of the importance of horizontal resolution, convective parameterization and radar data assimilation. In addition, we compare numerical weather forecasts to Lagrangian persistence, radar-based nowcasts.

2. DATA

2.1 *Verification data*

The verification data consists of maps of hourly rainfall accumulations derived from the 2D US composite radar reflectivity mosaics at 2.5km altitude (obtained from National Severe Storm Laboratory; Zhang et al., 2005), by applying a standard *Z-R* relationship, $Z=300R^{1.5}$, and accumulating instantaneous rainrate maps with a 10-minute temporal resolution.

2.2 *Model forecasts*

The first set of forecasts was generated by the GEM (Global Environmental Multiscale; Mailhot et al., 2006) model and is described by Surcel et al. (2009).

The remainder of the forecasts comes from the two control runs (from now on referred to as CN and C0) of the CAPS (Center for Analysis and Prediction of Storms) Storm-Scale Ensemble Forecasting (SSEF) system, run as part of an experimental forecasting program from April to June 2008 at NOAA's Hazardous Weather Testbed (HWT; Xue et al., 2009). The 10-member, WRF-based system produced 30 hour-forecasts starting at 00 UTC. Nine of the members assimilated radar observations of reflectivity and radial velocity using a CAPS 3DVAR system. The two control runs analyzed here do not have SREF-based perturbations and have identical model configurations, with the only difference being the assimilation of radar observations in CN and not in C0.

The main differences between the model runs are summarized in Table 1, and more information on the forecasting systems can be found in Mailhot et al. (2005) and Xue et al. (2009).

Model	GEM	SSEF
Reference	Mailhot et al., 2006	Xue et al., 2009
Horizontal resolution	15 km	4 km
Initial conditions	Regional data assimilation system	NAM 12UTC Radar data assimilation in CN
Cumulus parameterization	Kain-Fritsch/Kuo transient	none

Table 1. Model characteristics.

2.3 *Radar-based nowcasts*

MAPLE (see a complete description in Germann and Zawadzki, 2002) is an extrapolation-based technique for precipitation nowcasting. It uses the variational echo tracking method (VET; Laroche and Zawadzki, 1995) to estimate the motion field of precipitation, and a semi-Lagrangian backwards algorithm to extrapolate reflectivity maps to generate the forecasts.

Here, we have run MAPLE using the NSSL 2.5-km reflectivity maps to generate, every hour, 8-hour forecasts with a resolution of 2 km in space and 15 minutes in time.

2.4 *Case studies and analysis domain*

The analysis focused on 25 days from 16 April 2008 to 06 June 2008, when forecasts from all model configurations were available. The spatial domain (black rectangle in Fig. 1) was chosen to cover most of central and eastern United States, running from 103 W to 78 W in longitude and between 32 N and 45 N in latitude, in order to avoid the region around the Rocky Mountains where the quality of radar observations is poor.

* *Corresponding author address:* Madalina Surcel, McGill University, Dept. of Atmospheric and Oceanic Sciences, Montreal, Canada; e-mail: madalina.surcel@mail.mcgill.ca.

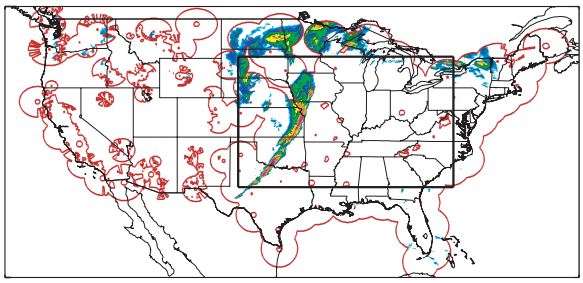

Fig. 1. Analysis domain. The red contours represent the coverage of the 2.5 km CAPPI maps, while the black rectangle extending between 103W and 78W in longitude and 32N and 45N in latitude corresponds to the domain on which all statistics are computed. The precipitation pattern observed in this figure is typical for spring 2008.

3. THE DIURNAL CYCLE DURING SPRING 2008 FROM PRECIPITATION FORECASTS

Figure 5 shows the diurnal cycle of average hourly rainrate during spring 2008 on a Hovmöller diagram, for observations, GEM, C0, CN and MAPLE. For the model forecasts we have considered forecast hours 0-23, and MAPLE was initialized at 00 UTC, 08 UTC and 16 UTC.

The models depict the observed propagating signal (diagonal rainfall band running from 103W at 19 UTC to 85W at 00 UTC; Fig. 2a), but they show more variability in propagating paths (the model-simulated bands are wider than observed; Figs. 2b-d). This could be due to the fact that precipitation forecasts suffer of positional and timing errors, and hence the model-simulated streaks are offset with respect to the observed. The spin-up time is visible in Figs. 5b and c in the case of GEM and C0, causing an absence of a maximum at 00 UTC along longitude 103W. The spin-up time also causes the discontinuity at 00 UTC in Figs. 5b and c, underlining the difference in forecast quality between lead times 0 and 23. Thanks to the radar data assimilation, CN does not suffer of these issues.

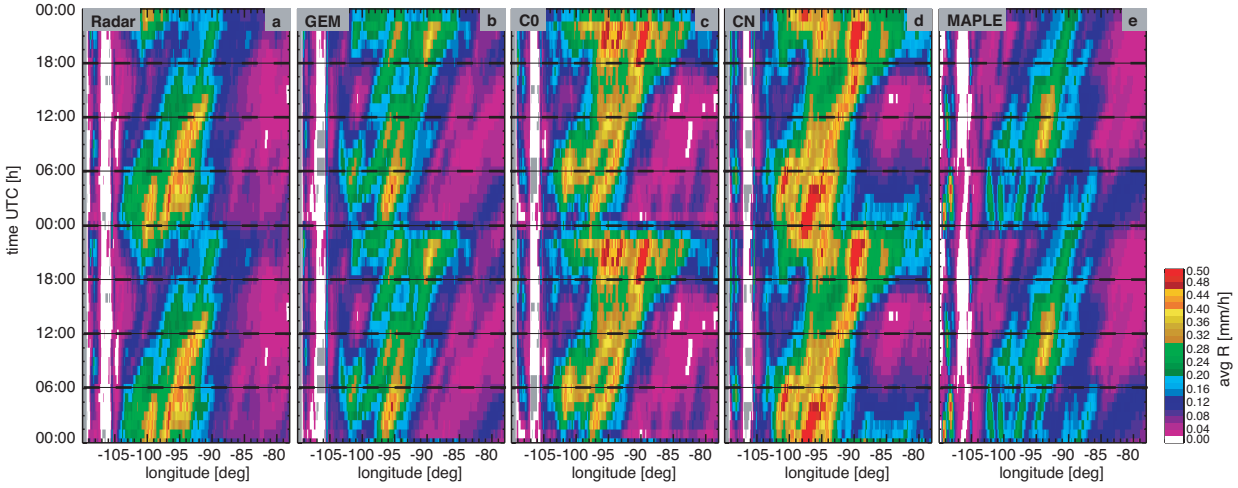

Fig. 2. Average diurnal cycle of precipitation intensity for the period 16 April 2008 to 06 June 2008 for radar observations (a) GEM (b), C0 (c), CN (d) and MAPLE (e). Units are mmh^{-1}.

We have also analyzed the ability of MAPLE to reproduce the diurnal cycle of precipitation (Fig. 5e). As explained by Surcel et al. (2009), and illustrated in Fig. 2a, there are two mechanisms of rainfall occurrence over the Continental US: initiation, along the foothills of the Rockies (longitude 103W) and propagation, in the longitudinal range 103W to 90W. As MAPLE is based on Lagrangian persistence (i.e., it takes the observed rainfall maps at initialization time and extrapolates them according to the estimated motion field, leaving in this way the intensity of the precipitation field constant along the forecast), it is able to depict the part of the diurnal cycle that is merely explained by steady propagation of the systems (which Germann et al., 2006, explained as a combination of steering level winds and apparent motion resulting from systematic growth and decay), but not the part associated with initiation and decay. This is evident in Fig. 2e. Being initialized at 00 UTC, a time of precipitation initiation, MAPLE nowcasts have little skill during hours 00-07 UTC. On the other hand, MAPLE does a better job than the NWP models in the 08-12 UTC time window, when the main mechanism of precipitation occurrence is propagation. Therefore, MAPLE's performance is highly dependent on initialization time, and initializing it at times when precipitation systems are well organized (for example every eight hours starting at 02 UTC, not shown), would improve its depiction of the diurnal cycle.

Figures 3 and 4 show, respectively, the power spectra of the Hovmöller diurnal cycles of average rainrate in Fig. 5 and the phase of the 24-hour harmonic as a function of longitude.

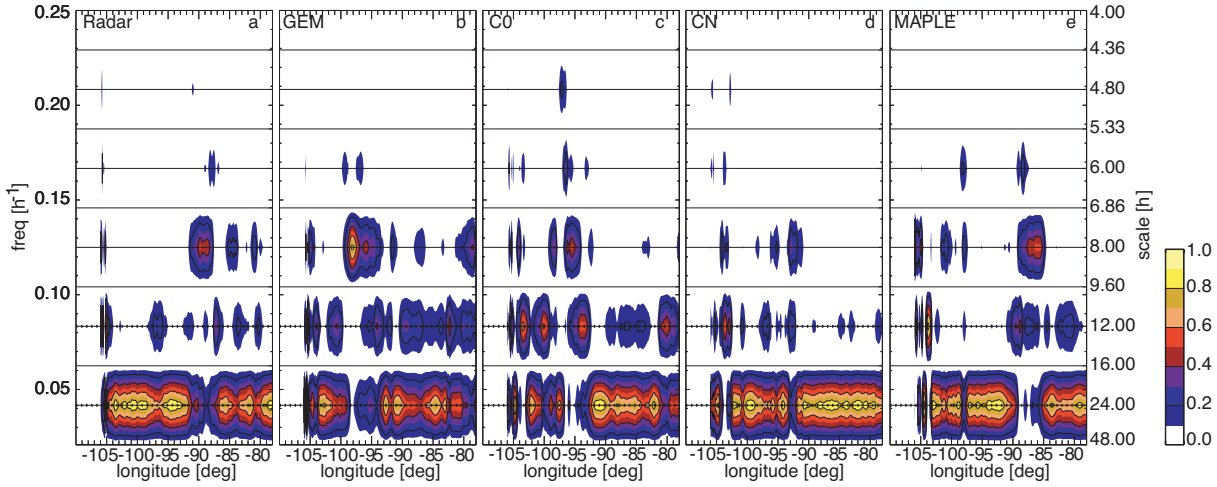

Fig. 3. Normalized power spectra corresponding to the diurnal cycles of average hourly rainrate of Fig. 2.

Indeed, the models, especially GEM and C0 show a weaker diurnal signal than observed (there is power associate with the 12- and 8-hour harmonics, Figs. 3b and c). CN reproduces best the observed power spectrum, showing that radar data assimilation has a stabilizing effect on the forecasted systems, as it corrects for positional errors at initialization time. The propagation speed, determined by the gradual shift of the phase of the 24-hour harmonic with longitude (Fig. 4) is best depicted by GEM and worst by C0. MAPLE forecasts capture the propagation of the precipitation systems in the 93W-90W longitudinal range, but with a systematic 2-hour delay.

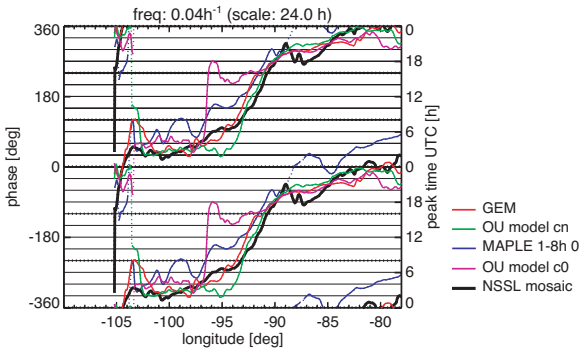

Fig. 4. Phase of the 24-hour harmonic as function of longitude corresponding to the average Hovmöller diagrams of Fig. 2 for rainfall accumulations. Different lines correspond to radar observations (thick black line), models (CN in green, C0 in magenta, GEM in red), and MAPLE (blue). The dotted lines indicate that the harmonic does not explain 10% of the observed variance.

4. OBJECTIVE EVALUATION OF PRECIPITATION FORECASTS

We have investigated the diurnal variability of forecast skill for models and MAPLE, in terms of the Critical Success Index (CSI, Wilks, 1995) and correlation (Fig. 5) between forecasts and observations. Here, the correlation coefficients were computed in logarithmic units and without subtracting the mean (as in Germann and Zawadzki, 2002).

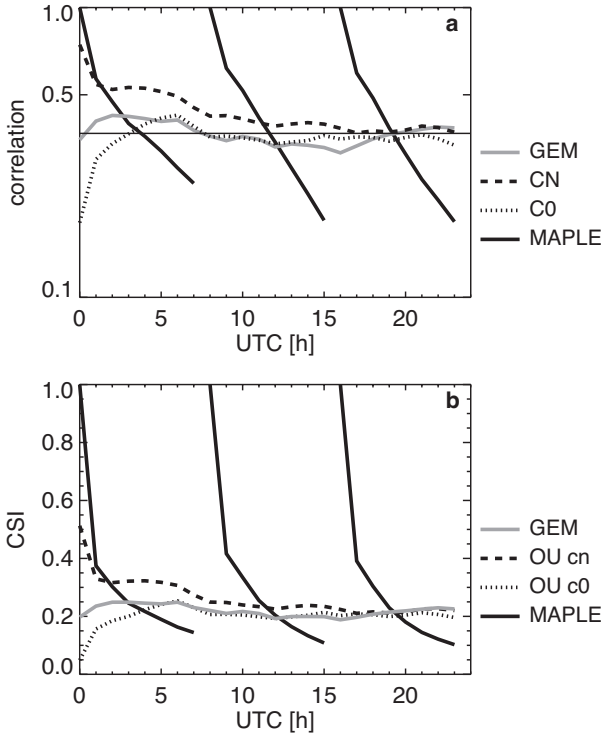

Fig. 5. Overall performance of the models as a function of time of the day. (a) correlation of the equivalent reflectivity fields (in dBZ); (b) Critical Success Index for the intensities over 0.2 mm/h.

CN performs better than C0 throughout the forecast, showing that radar data assimilation at initialization time has a beneficial impact on the average quality of the forecasts. On the other hand, it appears that increasing horizontal resolution beyond 15 km does not have any effect on forecast quality, as GEM is better, or at most equal to C0 at all times. However,

there are some observations to be made. First, the two models are not identical, and therefore the differences between them may come not only from their horizontal resolutions, but also from the quality of their physical representation. For example, it seems that C0 has a longer spin up time than GEM (roughly, 2 hours compared to 6), which can be due to the fact that the initial conditions for C0 are simply provided by the NAM analysis, while for GEM, they are provided by a 3D-VAR, regional data assimilation system. Then, C0 is expected to perform better than GEM during the summer, when precipitation is organized at the mesoscale, therefore demanding a high enough horizontal resolution to allow the explicit treatment of convection. Unfortunately, as the SSEF system is not run on a regular basis, it was not possible to evaluate it during a summer period.

MAPLE nowcasts show perfect CSI and correlation at initial time, but which quickly decay with lead-time. This decrease is steeper than observed by previous studies (Germann and Zawadzki, 2002), probably because our data set is not strictly composed of large scale, fairly predictable systems, but it includes convective cases in which MAPLE has little skill. In addition, the time it takes for the models to outperform MAPLE is lower in our case (2 hours for CN, 3-4 hours for GEM and C0) than found by Lin et al. (2005; 6 hours). This is also due in part to our data set, and to the better quality of the models (e.g. CN was run at higher resolution and had radar data assimilated).

For the model forecasts, other than already mentioned, CSI and correlation do not exhibit any significant dependence on the time of day. Therefore, it seems that the diurnal cycle of precipitation is not the main cause for the poor model performance.

It is worth mentioning two problems associated with this type of objective evaluation. First, as already mentioned, our data set is composed of precipitation cases that exhibit significant growth and decay. For these cases, MAPLE has little skill, being based on Lagrangian persistence. On the other hand, in verification against radar derived rainfall maps, MAPLE nowcasts have an advantage over model forecasts, as they are generated from radar observations. These two factors counteract each other.

5. CONCLUSIONS

In this paper, we have compared the ability of three NWP models to depict the diurnal cycle of precipitation over the continental US during spring 2008. We found that the analyzed NWP models could reproduce the propagating signal, showing however more variability in propagation paths than observed. CN performed best, especially at the beginning of the forecast time, showing the importance of radar data assimilation. Unfortunately, the little difference in performance between C0 and GEM did not show any beneficial effect of increasing horizontal resolution beyond 15 km.

We have also investigated the performance of MAPLE as a function of the time of day. As also suggested by previous studies (Berenguer et al., 2008), the diurnal cycle of precipitation strongly influenced MAPLE's performance, such that the quality of the nowcasts was highly dependent on the initialization time. Also, on average, for all precipitation cases during the study period, MAPLE nowcasts initialized at 00 UTC outperformed CN only during the first two forecast hours, suggesting the potential value of radar data assimilating NWP models for very-short term forecasting.

ACKNOWLEDGEMENTS

This work was made possible by the support of Environment Canada to the J. S. Marshall Radar Observatory.

REFERENCES

Berenguer, M., B. Turner, and I. Zawadzki, 2008: The effect of the diurnal cycle of precipitation in radar-based short-term forecasts. *5th European Conference on Radar in Meteorology and Hydrology*, Helsinki, Finland, CD-ROM P11.21.

Germann, U. and I. Zawadzki, 2002: Scale-dependence of the predictability of precipitation from continental radar images. Part I: Description of the methodology. *Monthly Weather Review*, **130,** 2859-2873.

Laroche, S. and I. Zawadzki, 1995: Retrievals of Horizontal Winds from Single-Doppler Clear-Air Data by Methods of Cross-Correlation and Variational Analysis. *Journal of Atmospheric and Oceanic Technology*, **12,** 721-738.

Laroche, S., P. Gauthier, J. St-James and J. Morneau, 1999: Implementation of a 3D variational data assimilation system at the Canadian Meteorological Centre. Part II: The regional analysis. *Atmosphere-Ocean*, **37,** 281-307.

Lin, C., S. Vasic, A. Kilambi, B. Turner, and I. Zawadzki, 2005: Precipitation forecast skill of numerical weather prediction models and radar nowcasts. *Geophysical Research Letters*, **32,** L14801.

Mailhot, J., S. Belair, L. Lefaivre, B. Bilodeau, M. Desgagne, C. Girard, A. Glazer, A. M. Leduc, A. Methot, A. Patoine, A. Plante, A. Rahill, T. Robinson, D. Talbot, A. Tremblay, P. Vaillancourt, A. Zadra, and A. Qaddouri, 2006: The 15-km version of the Canadian regional forecast system. *Atmosphere-Ocean*, **44,** 133-149.

Surcel, M., M. Berenguer, and I. Zawadzki, 2009: The diurnal cycle of precipitation from Continental radar images and Numerical Weather Prediction Models. Part I: Methodology and seasonal comparison. *Monthly Weather Review* (in review).

Turner, B. J., I. Zawadzki, and U. Germann, 2004: Predictability of precipitation from continental radar images. Part III: Operational nowcasting implementation (MAPLE). *Journal of Applied Meteorology*, **43,** 231-248.

Wilks, D. S., 1995: Statistical Methods in Atmospheric Sciences. 467.

Xue, M., F. Kong, K. W. Thomas, J. Gao, Y. Wang, K. Brewster, K. K. Droegemeier, J. Kain, S. Weiss, D. Bright, M. Coniglio, and J. Du, 2008: CAPS realtime storm-scale ensemble and high-resolution forecasts as part of the NOAA Hazardous Weather Testbed 2008 Spring Experiment. *24th Conference on Severe Storms*, American Meteorological Society, 12.2.

Zhang, J., K. Howard, and J. J. Gourley, 2005: Constructing three-dimensional multiple-radar reflectivity mosaics: Examples of convective storms and stratiform rain echoes. *Journal of Atmospheric and Oceanic Technology*, **22,** 30-42.